CHARACTERIZATION OF ALKYLSILANE SELF-ASSEMBLED MONOLAYERS BY MOLECULAR SIMULATION

Juan Manuel Castillo[1], *Mischa Klos*[2], *Karin Jacobs*[2], *Martin Horsch*[1*], *and Hans Hasse*[1]

[1]Laboratory of Engineering Thermodynamics, Department of Mechanical and Process Engineering, University of Kaiserslautern, Erwin-Schrödinger-Str. 44, 67663 Kaiserslautern, Germany

[2]Department of Experimental Physics, Saarland University, 66041 Saarbrücken, Germany

KEYWORDS

Self-assembled monolayers, dodecyltrichlorosilane, octadecyltrichlorosilane, molecular dynamics.

ABSTRACT

Self assembled monolayers (SAM) of dodecyltrichlorosilane (DTS) and octadecyltrichlorosilane (OTS) on silica are studied by molecular dynamics simulations at 298 K, 1 bar. The coverage (number of alkylsilane molecules per surface area) is systematically varied. The results yield insight in the properties of the alkylsilane SAMs, which complement experimental studies from the literature. Relationships are reported between thickness, tilt angle, and coverage of alkylsilane SAMs, which also hold for alkylsilanes other than DTS and OTS. They are interpreted based on the information on molecular ordering in the SAMs taken form the simulation data. System size and simulation time are much larger than in most former simulation works on the topic. This reduces the influence of the initial configuration as well as the periodic boundary conditions, and hence minimizes the risk of artificial ordering. At the same time, more reliable statistics for the calculated properties can be provided. The evaluation of experimental data in the field is often based on strongly simplified models. The results from the present work suggest that some of these lead to errors which could be avoided by introducing more realistic models.

INTRODUCTION

Self-assembled monolayers (SAMs) are widely used for modifying substrate surfaces. Bigelow *et al.*[1] first reported on self-assembled monolayers on a substrate in the late 1940s. The covalent binding of molecules to a suitable substrate and the self-assembly process leads to a very dense and robust monolayer. A large variety of surfaces can be modified by silane molecules, as for instance silicon[2], glass[3], metal[4], mica[5] or polydimethylsiloxane[6]. Depending on its end group, the silane transforms those substrates into hydrophobic or hydrophilic substrates. Silane SAMs on silicon wafers are a common model system because of their highly controllable properties. A dense silane monolayer forms an extraordinarily homogeneous surface, both chemically and topographically. By choosing the end group of the silane, the surface wettability can be tuned. A silane SAM with a hydrophobic tail group such as CH_3 on a formerly hydrophilic silicon-oxide surface, can result in water contact angles larger than 100°. At the same time, silane SAMs are mechanically robust and thermally stable up to at least 250 °C[7-9]. After silanization with a hydrophobic tail group, the surface tension is significantly reduced, and therefore these surfaces can be easily cleaned and handled, e.g. for studying adsorption of proteins or bacteria[10, 11], polymer dewetting[12], or selective area atomic deposition[13].

Lessel *et al.*[2] recently published a recipe for a wet chemical production process for silanizing silicon wafers with CH_3-terminated molecules such as dodecyltrichlorosilane (DTS) and octadecyltrichlorosilane (OTS). Although they provide insights into the surface parameters of the prepared silane SAMs, it is not clear how the silane molecules arrange on the substrate. In a recent study, Gutfreund *et al.*[14] developed a model for the molecular arrangement of the alkylsilanes based on X-ray scattering experiments. They employed an empirical three layer model to relate their experimental results to the molecular structure of the silane SAM, and found

that the actual height of the silane layer is lower than the theoretical length of an elongated silane molecule, from which they concluded that the silane chains are tilted with respect to the substrate. However, the main property that can be measured with X-ray scattering is the electron density, which does not provide direct information on molecular arrangement. The geometrical characteristics of silane SAMs on the nanometer scale determine their macroscopic properties. Although many authors characterized the surface properties of alkylsilane monolayers in terms of roughness, surface energy, and layer thickness using different experimental techniques[15-18], the description of the monolayer at molecular level is still lacking.

Simulation studies are able to characterize SAMs at molecular level by the use of molecular models or quantum chemistry calculations. Yamamoto *et al.*[19] performed Monte Carlo (MC) simulations of cross-linked OTS SAMs on silica, finding that the number of anchoring bonds is always much larger than the number of cross-linking bonds, and that cross-linking has a large effect on the lateral packing of the alkylsilane molecules. Zhang *et al.*[20] used ab-initio and molecular dynamics (MD) simulations at different temperatures to look for the optimal packing structure of OTS SAMs on silica, finding that intermediate packing densities have the lowest energy. Zhan *et al.*[21] performed MD simulations of hydroxilated alkylsilane SAMs on a planar silica substrate, showing that the molecular tilt angle is not only determined by coverage, but also by the specific molecular arrangement of the silane molecules on the substrate. Barlow *et al.*[22] observed that the bonded OTS layer on silica is essentially crystalline near the substrate, but more disordered and fluid-like far from it. Barriga *et al.*[23] ran MD simulations of OTS SAMs on silica at different high coverage, molecular arrangement of the molecules bonded to the substrate, molecular orientation, and temperature. The OTS molecules aligned nearly vertically due to close packing. In dense systems, different molecular arrangements led to large packing

energy differences. Finally, the tilt angles did not change with temperature, but gauche defects increased with increasing temperature. Dickie *et al.*[24] used geometric modeling techniques together with the rigid rod scanning method to map the packing potential energies of different silane SAMs on silica. They found that the interaction between CH_2 groups, which dominate the energy and geometry of the monolayers, increase the energetic stability of longer chains.

The tribological and wettability properties of alkylsilane SAMs on silica have also received much attention and were investigated by molecular simulation. For example, Chandross *et al.*[25] analyzed the influence of molecular disorder on the tribological properties of alkylsilane SAMs of different length, observing stick-slip motion at maximum coverage, which disappeared in disordered monolayers. Pastorino *et al.*[26] studied shear of a polymer between two silane SAMs using a coarse grained bead-spring model, finding fluid-like layering effects and a tendency of the molecules to align in the direction of the shear. Cione *et al.*[4] studied the deposition and wettability of ionic liquids on different tail-substituted alkylthiol and alkylsilane monolayers attached to gold and silica substrates. Hydroxyl-terminated surfaces decreased the attraction forces between the ions in the outer shells and reduced the local surface tension.

In this work, MD simulations of DTS and OTS alkylsilane monolayers on a silicon oxide substrate at ambient conditions (298 K, 1 bar) are performed. The resulting trajectories are used to analyze molecular arrangement of the alkylsilanes in the monolayers. Different monolayer properties are determined from simulation data and compared to experimental results, finding relationships between thickness, tilt angle and coverage, and revealing the underlying molecular ordering. It is shown that the detailed information provided by molecular simulations is also interesting for evaluating experimental data. It could replace some of the crude, oversimplified models which are presently used for that purpose.

SIMULATION DETAILS

MD simulations in the isobaric-isothermal ensemble (NPT)[27] were performed for different DTS and OTS self-assembled monolayers on silicon oxide at 298 K and 1 bar with the Gromacs simulation package[28], version 4.6.2. The supporting substrate was modeled as a flat β-cristobalite (1 0 1) surface (placed normal to the *y* axis) with the dimensions (11.5 x 11.1) nm^2 and thickness of about 2.3 nm. Cristobalite is commonly used as a model substrate for this type of systems instead of an amorphous SiO_2 surface[4, 29], as the order of amorphous SiO_2 films on silicon is similar to the cristobalite structure[30]. The superficial hexagonal arrangement of oxygen atoms in cristobalite, and the superficial oxygen-oxygen distance, are similar to those for amorphous silica[31]. The simulation box length was 10 nm in the direction perpendicular to the surface. This value was chosen to avoid interactions of the monolayer with the periodic image of the bottom side of the substrate. The cristobalite atoms were initially placed at their crystallographic positions[32]. The density of surface reactive groups (silanols, i.e. –Si-OH) is 5.52 groups/nm^2, which is also the maximum density of silane substituents on the selected cristobalite substrate. The number of substituents per surface area is called coverage in the following, and measured in units of nm^{-2}. To obtain alkylsilane SAMs with coverage between 1.0 and 5.52 nm^{-2}, the corresponding number of DTS or OTS molecules was bonded to randomly selected oxygen atoms on the top side of the substrate. Every bonded molecule was initially placed perpendicular to the surface in a random orientation and an all-trans conformation. Different alkylsilane SAMs generated randomly with this procedure and the same coverage produced the same results within the error bars of the simulation. Figure 1a shows a view of the superficial oxygen atoms of the substrate, indicating which of these atoms are bonded to alkylsilane molecules in one simulation of DTS at 4.5 nm^{-2} coverage. Figure 1b shows the arrangement of the DTS substituents after 20

ns simulation time. In Figure 2, the arrangement of DTS SAMs at 1.0, 2.5, and 4.5 nm^{-2} coverage is also shown. Periodic boundary conditions in all directions were used in the simulations. Theoretical analysis indicate that even at large coverage there are few, if any, multiple bonds of each molecule with the substrate, and a low number of cross linking bonds between silane molecules[19, 33]. Therefore, the study was limited to the simplest case: no cross-linking and one single covalent bond per molecule, where the rest of the chlorine atoms are substituted by OH groups. For molecular simulation results which include cross-linking, the reader is referred to the works of Osnis *et al.*[34] and Kong *et al.*[35]

The OPLS all-atom force field[36] was used for describing the atomic interactions, with additional potential parameters and partial charges for modeling the silica bulk[37]. Lennard-Jones potentials were truncated at a cutoff distance of 1.5 nm, and isotropic tail corrections (which contribute to the energy, but not to the force) were added to these potentials[27]. Electrostatic interactions were calculated with the Particle Mesh Ewald method[27] with a relative tolerance of 10^{-6}. The force field parameters and the potential functions can be found in the Supporting Information (Tables T1-T4). In the OPLS potential, the Lennard-Jones interaction between unlike atoms is defined by a geometric mixing rule in both the σ and the ε parameters[36]. The energy parameter ε_{ij} between unlike atoms *i* and *j* can be modified by a mixing factor ζ:

$$\varepsilon_{ij} = \zeta \cdot \sqrt{\varepsilon_{ii} \cdot \varepsilon_{jj}} \qquad (1)$$

The mixing factor was equal to 1, except in a series of simulations in which that factor was varied for all the interactions between the silane molecules and the substrate. The equations of motion were integrated using a leapfrog algorithm with a time step of 1 fs. The temperature of the system was kept fixed at 298 K using a velocity rescaling thermostat with a stochastic term[38]

and a time constant of 0.1 ps. The pressure was kept at 1 bar by using Berendsen pressure coupling[27] with a time constant of 0.5 ps. The initial system configuration, described previously, was first subjected to an energy minimization using the conjugated gradient method. Afterwards, velocities were assigned to each atom from a Maxwell distribution, and the system was equilibrated during 11 ns. Finally, production runs were performed for 10 ns. The trajectories generated in the production runs were analyzed to calculate system properties, and error bars were estimated using block analysis and considering simple standard deviations[27]. In simulations of large, complex systems like the present one, the relaxation time needed to reach equilibrium is large. Figure S1 in the Supporting Information shows that the relaxation time can exceed even the long simulation times of the present study. The remaining differences between the properties obtained in this work and the equilibrium properties are minor, and do not affect the discussion and conclusions presented here. As an example, system properties were calculated by ensemble average at different time intervals of several 40 ns long simulations, and the values obtained changed only slowly with time, and usually within the error bars (Table T5 in the Supporting Information).

Geometric properties that are commonly used to characterize silane SAMs were determined by post-processing the MD trajectories. This includes the thickness, the roughness, the gauche factor, the radius of gyration (R_g), the superficial radial distribution function (RDF), the electron density profile, distance autocorrelations, and molecular orientation. The relative value of a property is defined as the property divided by the maximum value it can take. The roughness is defined as the standard deviation of the thickness[35], and the gauche factor as the number of torsions in the molecule that differ more than ten degrees from 180º (trans torsion), divided by the total number of torsional degrees of freedom[20, 23]. The electron density was calculated

assuming a Gaussian distribution of electrons over the characteristic length scale corresponding to the atomic van der Waals radius[39].

The carbon beads of the alkylsilane molecules were numbered consecutively, bead 1 being the carbon atom bonded to silicon, and bead 12 and 18 the terminal carbon atoms of DTS and OTS, respectively. The definitions of the tilt angle α, the twist angle β, and the orientation angle γ, are illustrated in Figure 3. Details on R_g, the superficial RDF, the distance autocorrelation, and the angle histogram can be found in the Supporting Information.

RESULTS AND DISCUSSION

Thickness

The silane SAM layer thickness measured by different experimental methods, such as ellipsometry analysis, X-ray reflectivity, or infrared dichroism, show contradicting values in the measured layer thickness[40]. There is some discussion on how to interpret the experimental layer thickness from an atomistic point of view. The layer thickness is often considered to be the average distance between the oxygen atom of the substrate bonded to the alkylsilane molecule and the atom of its hydrocarbon tail further from the substrate, projected in the direction normal to the surface. With this definition, the maximum layer thickness for OTS SAMs on SiO_2 (completely vertical, all-trans molecules), derived from standard bond lengths, atomic covalent radii, and van der Waals radii[41], is generally accepted to be 2.62 nm (1.863 nm for DTS). This layer thickness is slightly larger than the maximum layer thickness possible with the model used in this work (2.54 nm, 1.77 nm for DTS). Curiously, some authors have reported experimental layer thicknesses for OTS SAMs of 2.95 ± 0.15 nm, 2.8 nm, and 3.0 ± 0.2 nm, which are larger than these values[16, 42, 43]. There are different possible causes which can be difficult to determine, such as a poor estimates of the reflectivity index, or incomplete removal of non-attached molecules after synthesis. Experimental studies at high coverage report layer thicknesses between 2.4 and 2.7 nm for OTS[2, 4, 15, 17, 18, 29, 44-47]. Less data are available for DTS, for which the layer thickness is reported to be about 1.4 nm by Cione *et al.*[4] and Booth *et al.*[29], and 1.8 nm by Lessel *et al.*[2].

It is also possible to consider the thickness of the hydrocarbon chain of the molecules, or tail thickness. The tail thickness is equal to the average distance normal to the surface between the

silicon atom of the alkylsilane molecule, and the atom of its hydrocarbon tail further from the substrate. With this definition, the tail thickness h_t is always smaller than the layer thickness. In the OPLS model, the maximum tail thickness $h_{t,max}$ is 1.49 nm for DTS and 2.25 nm for OTS. Figure 4 compares the relative DTS and OTS tail thickness $h_t/h_{t,max}$ as a function of coverage c, obtained by simulation, with experimental data. The thickness increases with coverage, as it has been demonstrated experimentally[29]. It has been shown that, at a given coverage, the monolayer thickness increases linearly with the alkylsilane chain length[4, 41]. Therefore, it is not surprising to find that the relative tail thickness as a function of coverage is independent of the particular type of alkylsilane. The data obtained in the present study was fitted to a quadratic law,

$$\frac{h_t}{h_{t,\max}} = -0.117 + 0.370 \cdot \left(\frac{c}{nm^{-2}} \right) - 0.031 \cdot \left(\frac{c}{nm^{-2}} \right)^2 \quad (4)$$

This equation is not valid for coverages below 1 nm^{-2}. It can be used to estimate coverage, which is a parameter difficult to determine accurately in experiments, when the tail thickness of an alkylsilane monolayer is known. Tidswell *et al.*[48] measured an OTS tail thickness of 2.13 ± 0.05 nm in a SAM on silica with coverage of 4.5 ± 0.3 nm^{-2}, which perfectly matches the simulation data obtained in this work. The simulation results are also consistent with the data of Lessel *et al.*[2] for alkylsilane SAMs with coverage larger than 4 nm^{-2}. A parallel study was done considering the layer thickness of the monolayer instead of the tail thickness, showing again excellent agreement between the calculated layer thickness and both experimental and previous simulation data (Figure S2 in the Supporting Information).

Tilt angle

Experimentally, the tilt angle is usually indirectly determined from the relative thickness of the monolayer. This method is not very precise, especially at the small angles found at large coverage[49]. Experimental studies have found that there is a strong dependence of the molecular tilt angle on the type of substrate, but only if the substrates are composed of different chemical species[44, 50, 51]. It is clear that the tilt angle is directly related to coverage[42], and there have been attempts to find an explicit relationship between these properties[15]. Figure 5 contains the present simulation results, which shows a clear quadratic dependence of the tilt angle α, measured in degrees, on coverage c,

$$\alpha = 107.99 - 29.47 \cdot \left(\frac{c}{nm^{-2}} \right) + 1.86 \cdot \left(\frac{c}{nm^{-2}} \right)^2 \quad (5)$$

Again this equation is not valid at coverages below 1 nm^{-2}. As before, it is found that an important property of the layer, in this case the tilt angle, does not depend on the length of the alkylsilane molecule. Therefore, differences in the tilt angle between DTS and OTS molecules in experiments performed at similar conditions should be explained by differences in coverage[2, 14]. Experimental data at high coverage indicate a tilt angle lower than 20 degrees for OTS[2, 14, 15, 41, 44, 46, 48, 52], in complete agreement with the simulation results. The present simulations perfectly match the simulation results of Kaushik *et al.*[53], although they provide a tilt angle around 10 degrees smaller than experiments with known coverage. On the other hand, the simulated tilt angle is lower than 15 degrees at the highest coverage, in agreement with the experimental work of Tillman *et al.*[46]. The simulation results of Barriga *et al.*[23] at different coverage show very small tilt angles, contradicting experimental observation. Therefore, they are not included in Figure 5. Zhan *et al.*[21] found by molecular simulation that the tilt angle not only depends on coverage, but also on the grafting pattern on the substrate. It might be possible that their

simulations were too short (properties averaged over 250 ps), or their system too small (36 alkylsilane chains on a 2.748 x 2.954 nm^2 surface).

A quadratic relationship is also found between the relative tail thickness and the tilt angle (Figure S3 in the Supporting Information). If the alkylsilane chains were completely rigid, the curve describing this relationship should be the arccosine function. In fact, most experimental data follow this trend because the tilt angle is calculated from the ellipsometry-measured tail thickness under the former assumption. This may explain the differences of around 10 degrees found between the experimental and simulated tilt angles.

Radius of gyration and gauche factor

It is well known that alkylsilane SAMs stay mainly in an all-trans conformation[44, 51, 52]. The relative radius of gyration (Figure S5 in the Supporting Information) increases with increasing coverage, and it is always larger than 0.85, which corresponds to largely stretched molecules. At the same time, the number of gauche defects decreases with increasing coverage (Figure S6 in the Supporting Information). A concentration of gauche defects at the terminal carbon atoms is found (Figure S7 in the Supporting Information). This has been previously observed both experimentally and by molecular simulation[20, 44, 54]. As OTS has a larger number of carbon atoms in the middle of the hydrocarbon chain than DTS, which is where the minimum number of gauche defects is observed, the average gauche factor is lower for OTS than for DTS.

Roughness

Experimental values between 0.1 nm and 0.3 nm have been reported for the roughness of OTS and DTS monolayers at complete or very high coverage[2, 14, 42, 45], which is consistent with the

simulation results shown in Figure 6. It is important to note that the maximum coverage reachable experimentally is of the order of 4 to 5 nm^{-2}, as consistently reported in the literature [41, 48]. The OTS roughness is always larger than the roughness of DTS except at very high coverage, which is also in agreement with experimental data[2]. As OTS is a longer molecule than DTS, the differences in local thickness can be larger. The roughness has a maximum at intermediate coverage, and the OTS maximum occurs at lower coverage than for DTS. Experimental roughness measurements have to be analyzed with care, as it has been argued that they may depend on the immersion time during synthesis, even when the times are long enough to generate complete monolayers[42]. A plot of the layer thickness as a function of the carbon bead reveals that the height increases monotonically with the carbon bead number (Supporting Information, Figure S9). This indicates that the molecules do not bend back to the substrate. For extended information on structural monolayer properties (superficial radial distribution, autocorrelation, angle histograms), the reader is referred to the Supporting Information.

Influence of the alkylsilane-substrate interaction

A study was performed, in which the mixing factor ζ defined in Equation (1) was varied between 0.1 and 1.4 for the interactions between the alkylsilane molecules and the substrate. In Figure 7, the results for the layer thickness are plotted as a function of the mixing factor at low and high coverage. At high coverage, there is hardly any influence of the mixing factor on the layer thickness, as the molecules arrange approximately perpendicular to the substrate and interact weakly with it. Even at low coverage, the influence of the mixing factor in the layer thickness is only large when the mixing factor differs more than 50% from unity. When the mixing factor decreases, the layer thickness increases, as the alkylsilanes stick less to the substrate. Howevery, typical values of the mixing factor that have been adjusted to reproduce experimental data, e.g.

for vapor-liquid equilibria, are rarely smaller than 0.8 or larger than 1.2. The conclusion is that the inter-chain interactions determine the geometrical properties of the monolayer, in agreement with results derived from experimental data[15, 42], and previous simulation studies[24, 54].

Electron density

The electron density as a function of the height normal to the surface can be obtained from reflectivity data by fitting to a multilayer model[55]. Figure 8 shows the electron density as a function of the coordinate perpendicular to the surface (y coordinate in the simulation) at different coverage obtained from the simulations in the present work. The value of the *y* coordinate at the origin is selected to be located at the center of the SiO_2 substrate in the simulation. The electron density of the monolayer in the vicinity of the substrate is similar for DTS and OTS, as at that location there is no difference between the molecular geometry of both systems. At high coverage, the electron density has a plateau at intermediate distances to the substrate before falling to zero. The width of the plateau is larger for OTS than for DTS, and the electron density falls to zero at longer distances from the substrate at the same coverage. This can be explained by the larger size of OTS relative to DTS molecules. The drop to zero in the electron density occurs at larger distances from the substrate at increasing coverage, the width of the plateau and its height slightly increase. This is a direct consequence of the decreasing tilt angle with increasing coverage. The drop to zero takes place at distances larger than the layer thickness because the electron distribution is described by Gaussian functions. The electron density inside the substrate slightly decreases with increasing coverage, and increases at the

substrate boundary. This is probably an artifact of the simulation, created by a substrate model which overestimates the isothermal compressibility of silica.

The simulation data are compared to the experimental electron density obtained by X-ray reflectometry[2] in Figure 9. The *y* coordinates of the electron density from simulation and experiment were matched by comparing the electron density profiles in the alkyl tail regions (which are the most sensitive regions of the electron density with respect to coverage), regarding simulations at different coverage. The best match was obtained assuming 3.75 nm^{-2} coverage for DTS, and 4.5 nm^{-2} for OTS. This is in agreement with experimental results, which show that the alkylsilane chain length that provides an optimal molecular order in alkylsilane SAMs is close to the chain length of OTS[56]. Therefore, experimental OTS would in general have larger coverage than DTS SAMs prepared under the same conditions. The simulated electron density inside the SiO_2 material perfectly matches the experimental data (~ 690 e/nm^3).

Qualitatively, the experimental and the simulation results for the electron density agree in a large range of the *y* coordinate. The existence of a plateau for OTS and the absence of it for DTS are predicted by the simulation. Quantitative differences, which are particularly large close to the substrate interface, should not be over interpreted. The differences between the amorphous SiO_2 and cristobalite model could explain some of the differences in the electron density at the substrate interface. The larger height of the plateau in the experimental electron density may be explained by agglomerations of carbon atoms between the chains, or unbound carbon chains on top of the SAM, which would increase the electron density compared to the 'clean' simulation. Besides uncertainty in the simulation, the evaluation of the experimental data relies on a multilayer model, which assumes two different layers for the amorphous SiO2 substrate and the silane head group, and reference values of the refraction index for every layer. It is also difficult

to quantify the influence of surface roughness both in the simulation and in the experiment, which would affect the electron density mainly at the substrate interface.

CONCLUSION

Molecular simulations were performed to analyze properties of alkylsilane (DTS and OTS) monolayers on silica as a function of the coverage. Relationships are proposed for the relative monolayer thickness and the tilt angle as a function of the coverage, which are found to be independent of the alkylsilane chain length. The simulation results for the monolayer thickness and electronic density agree with experimental data. Deviations which are observed for the tilt angle probably result from invalid assumptions employed for evaluating the experimental data. While the trends of the experimental and simulated electron densities agree, the results do not match quantitatively. The deviations in this case are attributed to the simple layer model used to interpret X-ray reflectometry data. It would be interesting to include the more detailed information from the simulation in the evaluation of the experimental data. This will be the subject of future work.

Figure 1. a) Arrangement of the superficial oxygen atoms of β-cristobalite (101). The minimum oxygen-oxygen distance is about 0.44 nm. The oxygen atoms are either bonded to an alkylsilane molecule (black circles), or not (grey circles). b) Arrangement of alkylsilane molecules, represented as rigid sticks connecting the atom bonded to the substrate and the terminal group of the molecule. Both figure views were obtained from a MD simulation of DTS SAMs at 4.5 nm^{-2} coverage.

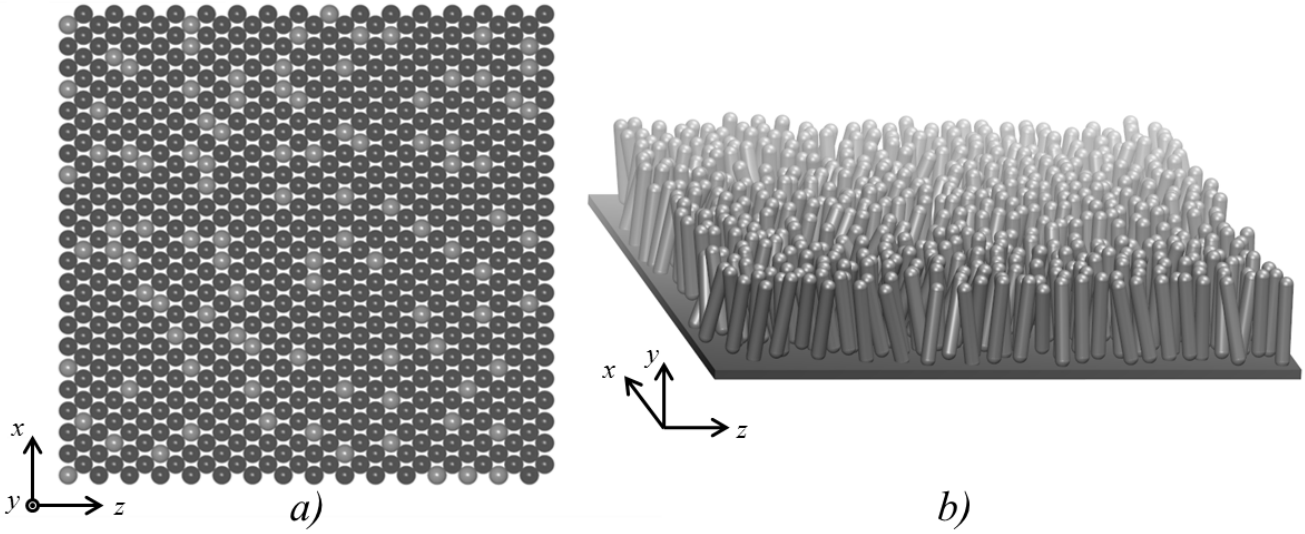

Figure 2. Arrangement of DTS alkylsilane molecules on a β-cristobalite (101) substrate, obtained by molecular simulation at different coverage: 1.0 (top), 2.5 (center), and 4.5 nm^{-2}. Red atoms, oxygen; yellow atoms, silicon; blue atoms, carbon; white atoms, hydrogen.

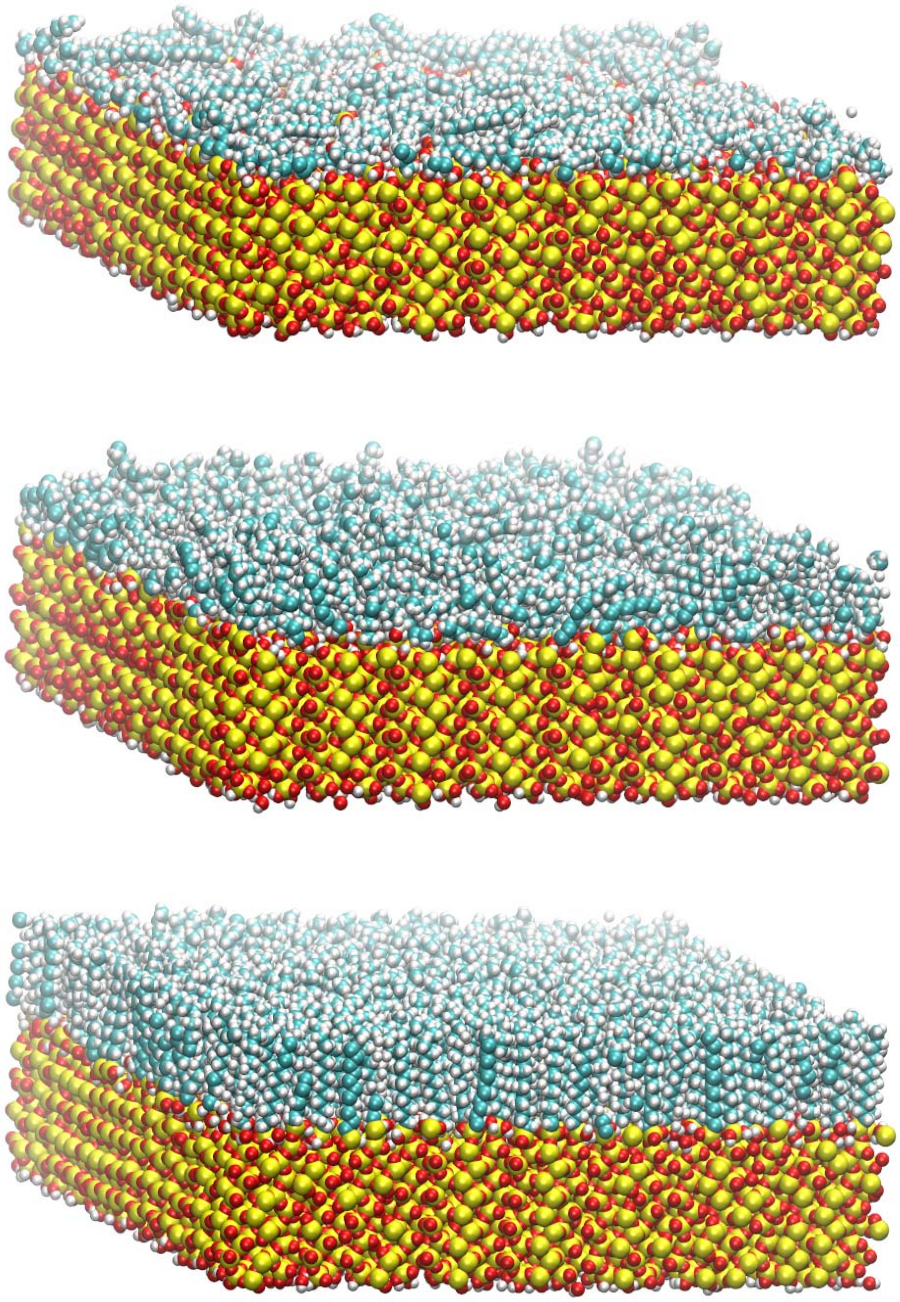

Figure 3. Geometric parameters describing the orientation of an alkylsilane molecule attached to a surface normal to the *y* axis, measured as a function of a selected carbon atom. The selected atom is marked by a white circle. The molecular axis for the selected atom is defined as the axis joining that atom with the silicon atom of the molecule. Black, carbon atoms; white, hydrogen atoms; grey, silicon atom. *h*, distance to the surface (see text for the different possible definitions of the thickness); α, tilt angle of the molecular axis with the normal to the surface; β, twist angle: rotational angle around the axis of the alkylsilane molecule, which is equal to zero when the distance of the first carbon bead to the surface is maximal; γ, orientational angle between the projection of the molecular axis on the surface and the *x* axis. By convention, all angles are defined counterclockwise, looking down from the substituents to the substrate.

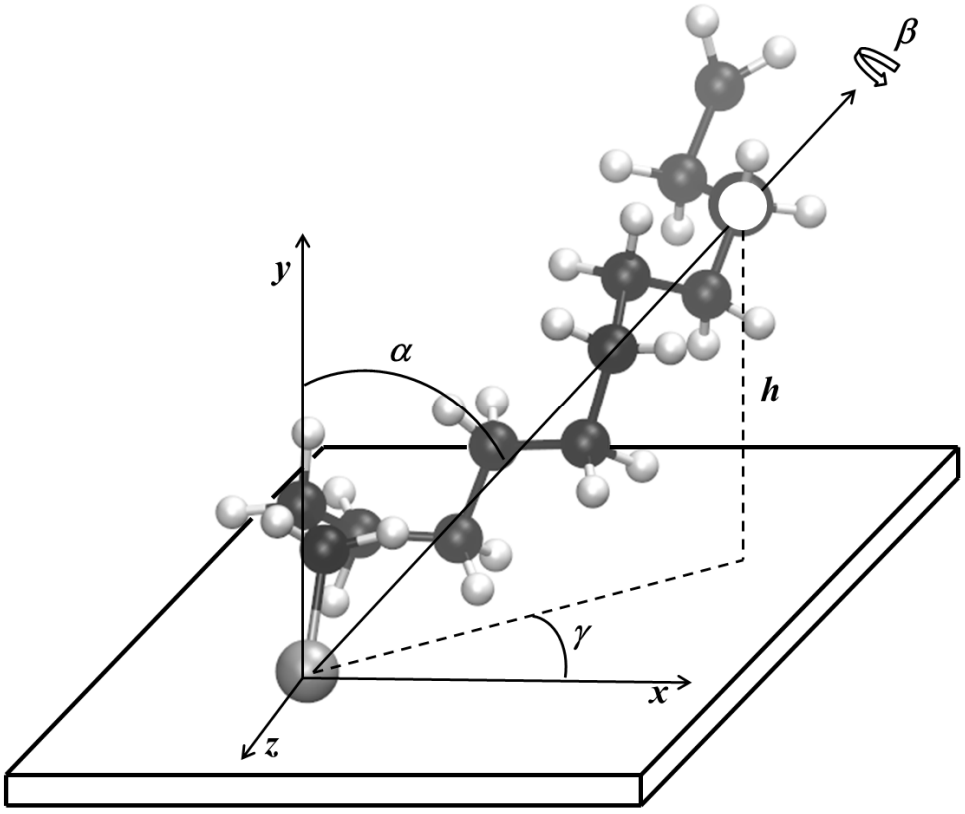

Figure 4. Relative tail thickness as a function of coverage. Results from molecular simulation for DTS (squares) and OTS (triangles), and experimental data for OTS[48] (circle); line, quadratic fit. Error bars for simulation data are within symbol size.

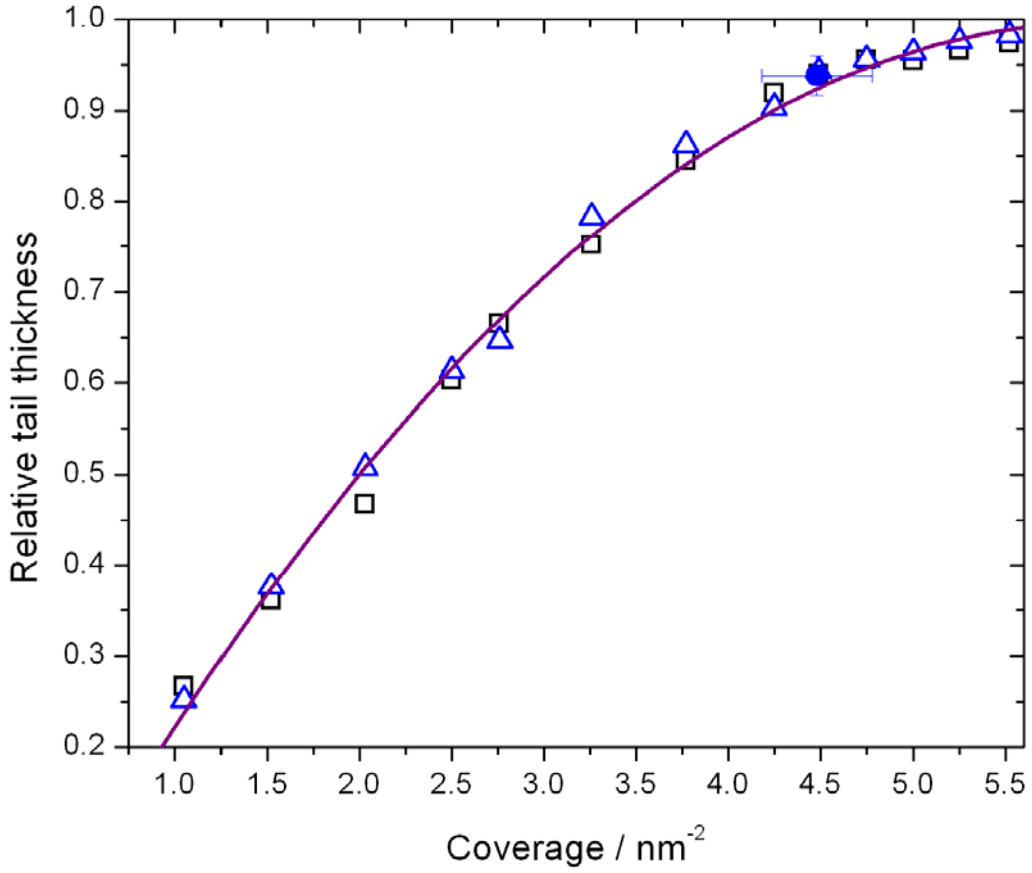

Figure 5. Tilt angle α as a function of coverage. Simulation data for DTS (squares) and OTS (triangles); line, quadratic fit. Error bars are within symbol size. Experimental (closed symbols) and other simulation (open symbols) data for OTS are also shown. Circle, Tidswell *et al.*[48]; diamond, Tillman *et al.*[46]; triangle pointing down, Kaushik *et al.*[53].

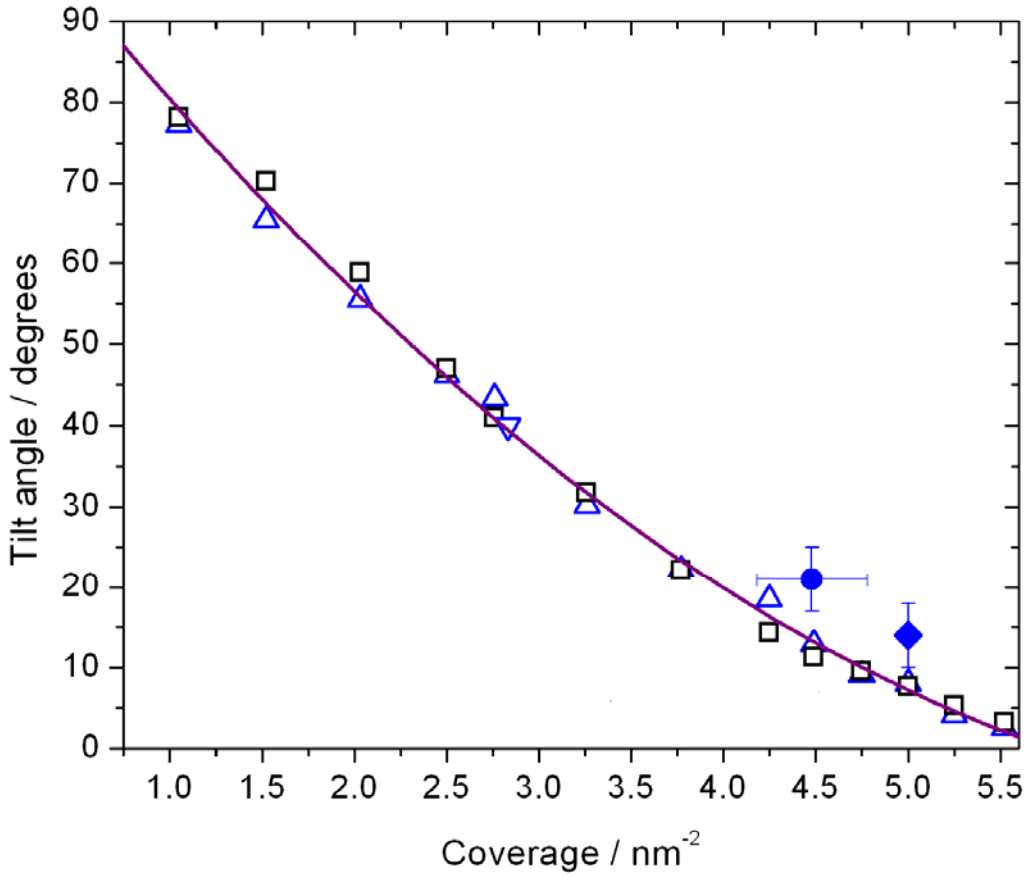

Figure 6. Surface roughness as a function of coverage. Simulation data for DTS (squares) and OTS (triangles). Error bars are within symbol size. Lines joining points are a guide to the eye.

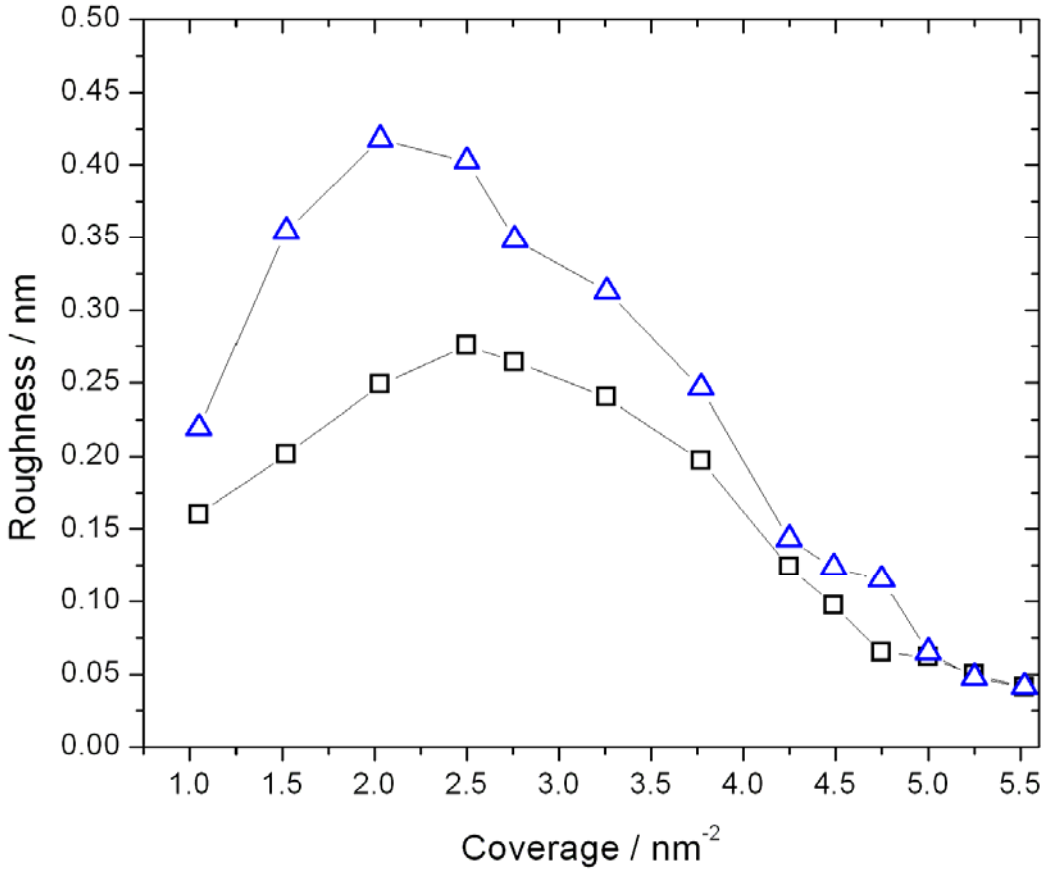

Figure 7. Layer thickness as a function of the mixing factor ζ. Results for DTS (squares) and DTS (triangles) at 4.5 nm^{-2} coverage (closed symbols) and 1.5 nm^{-2} coverage (open symbols). Error bars are within symbol size.

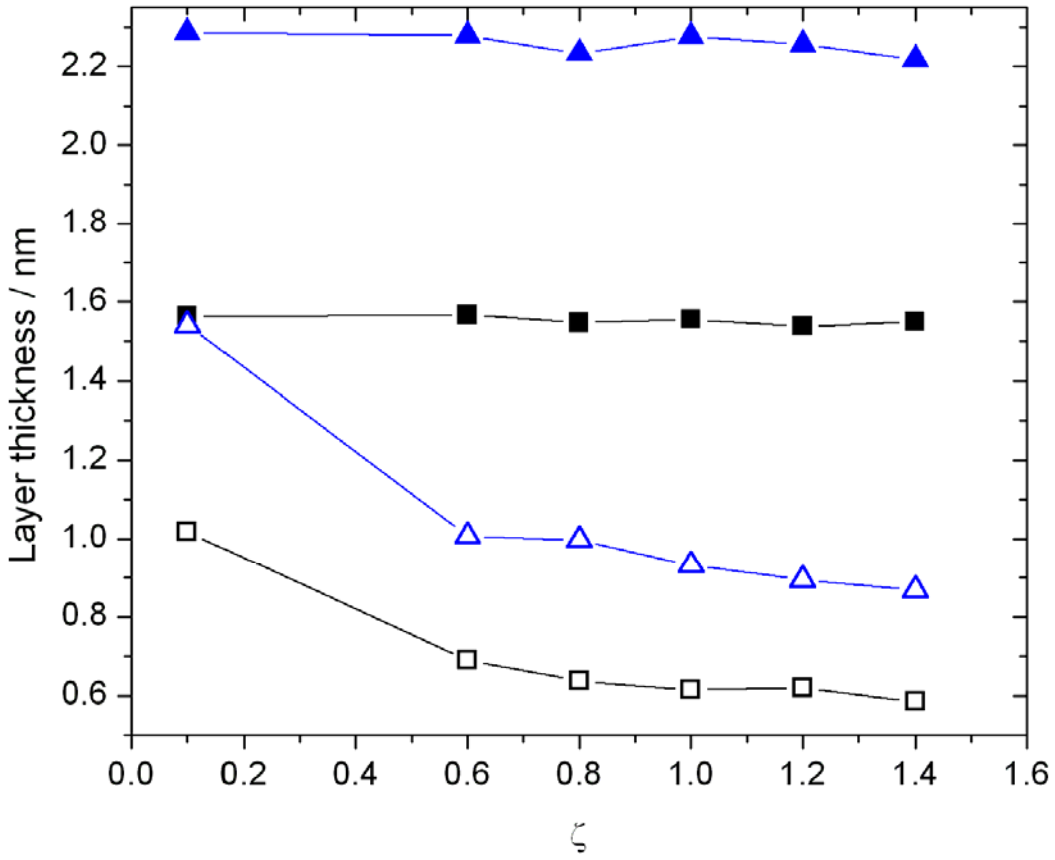

Figure 8. Electron density of SAMs, obtained by molecular simulation for DTS and OTS at different coverage: 1 nm^{-2} (solid line), 2 nm^{-2} (dashed line), 3.25 nm^{-2} (dotted line), 4.25 nm^{-2} (dash-dotted line), and 5.52 nm^{-2} (short dotted line).

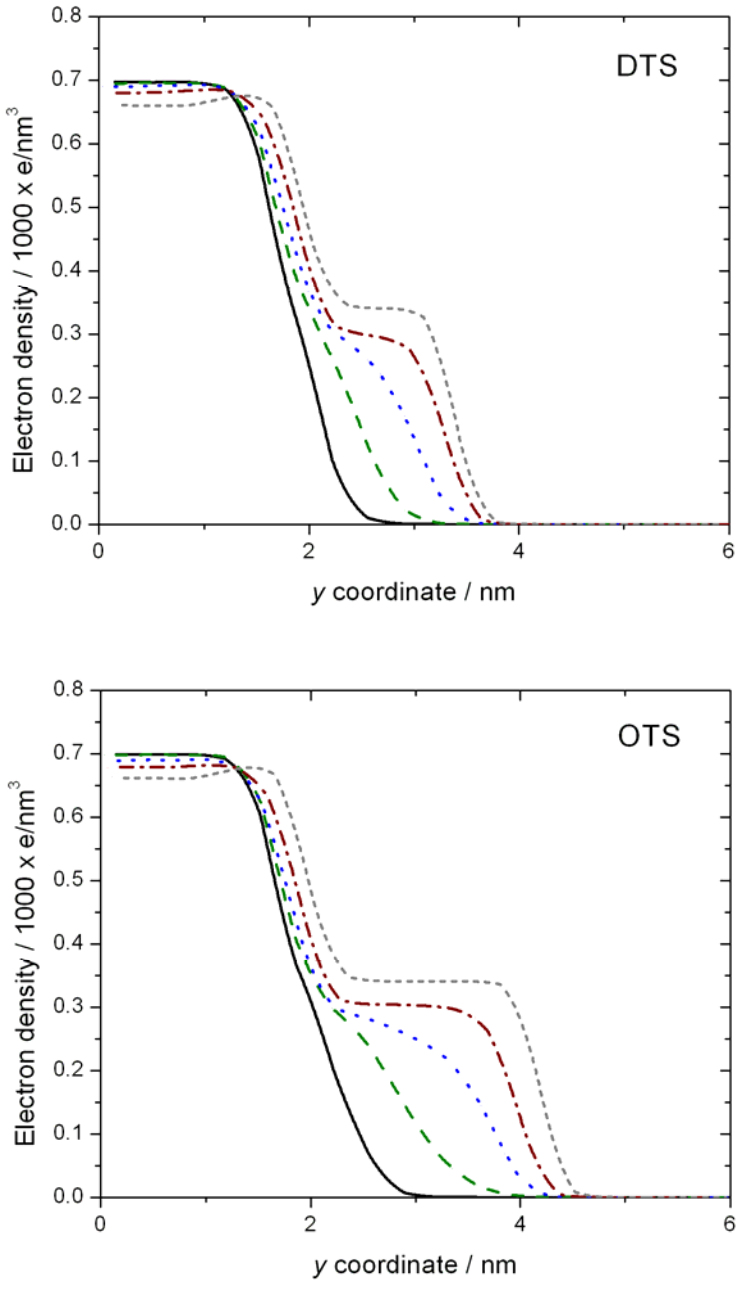

Figure 9. Simulated electron density. Squares, DTS at a coverage of 3.75 nm^{-2}; triangles, OTS at a coverage of 4.5 nm^{-2}; solid curve, experimental data for DTS[2]; dashed curve, experimental data for OTS[2].

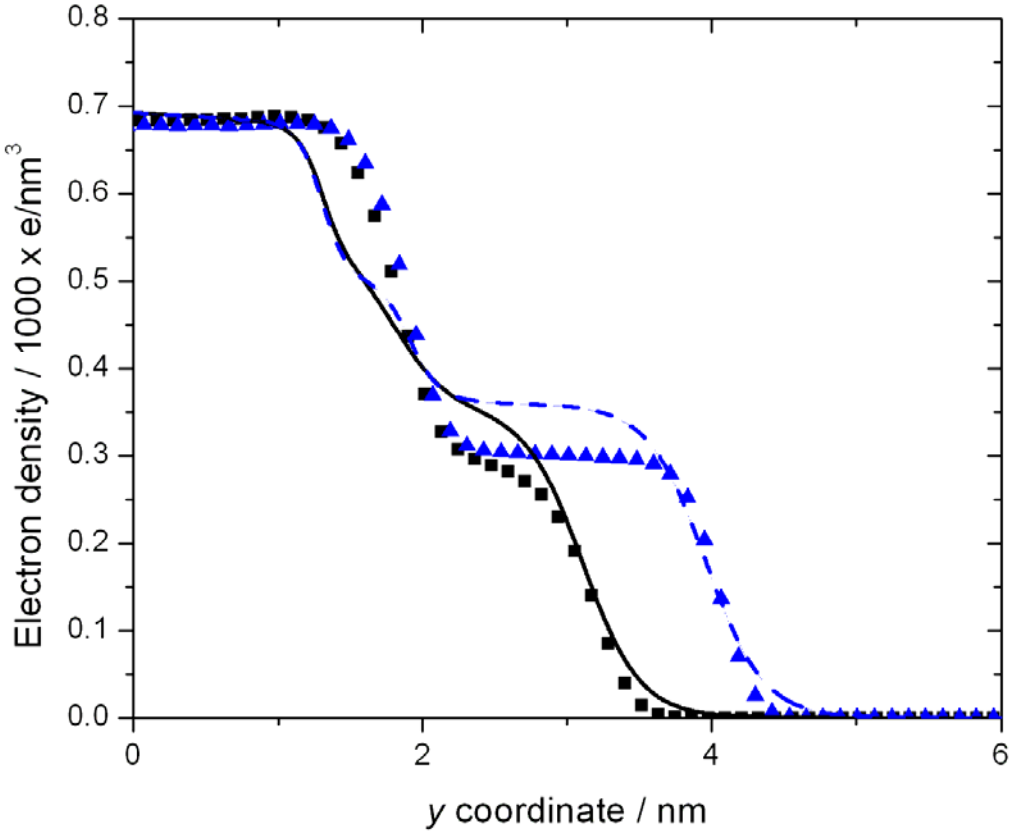

ASSOCIATED CONTENT

Detailed description of the force field parameters used in this work, numerical data used to plot the figures, graphs showing complementary results, and an extended discussion of those results. This material is available free of charge via the Internet at http://pubs.acs.org."

AUTHOR INFORMATION

Corresponding Author

*martin.horsch@mv.uni-kl.de

Author Contributions

The manuscript was written through contributions of all authors. All authors have given approval to the final version of the manuscript.

ACKNOWLEDGMENTS

The authors would like to thank S. Grottel and G. Reina for fruitful discussions, DFG for support within the Reinhart Koselleck program, and the SFB 1027 and GRK 1276 projects. The present work was conducted under the auspices of the Boltzmann-Zuse Society for Computational Molecular Engineering (BZS), and the MD simulations were performed on the Elwetritsch cluster at the Regional University Computing Center Kaiserslautern (RHRK) under the grant TUKL-MSWS.

ABBREVIATIONS

MD, molecular dynamics; MC, Monte Carlo; SAM, self-assembled monolayer; DTS, dodecyltrichlorosilane; OTS, octadecyltrichlorosilane; RDF, radial distribution function.

REFERENCES

1. Bigelow, W. C.; Pickett, D. L.; Zisman, W. A., Oleophobic monolayers. 1. Films adsorbed from solution in non-polar liquids. *Journal of Colloid Science* **1946,** 1, (6), 513-538.
2. Lessel, M.; Bäumchen, O.; Klos, M.; Hähl, H.; Fetzer, R.; Seemann, R.; Jacobs, K., Self-assembled silane monolayers: A step-by-step high speed recipe for high-quality, low energy surfaces. *arXiv:1212.0998* **2012**.
3. Eisert, F.; Gurka, M.; Legant, A.; Buck, M.; Grunze, M., Detection of molecular alignment in confined films. *Science* **2000,** 287, (5452), 468-470.
4. Cione, A. M.; Mazyar, O. A.; Booth, B. D.; McCabe, C.; Jennings, G. K., Deposition and Wettability of [bmim][triflate] on Self-Assembled Monolayers. *Journal of Physical Chemistry C* **2009,** 113, (6), 2384-2392.
5. Britt, D. W.; Hlady, V., An AFM study of the effects of silanization temperature, hydration, and annealing on the nucleation and aggregation of condensed OTS domains on mica. *Journal of Colloid and Interface Science* **1996,** 178, (2), 775-784.
6. Chaudhury, M. K.; Whitesides, G. M., Correlation between surface free-energy and surface constitution. *Science* **1992,** 255, (5049), 1230-1232.
7. Ding, J. N.; Wong, P. L.; Yang, J. C., Friction and fracture properties of polysilicon coated with self-assembled monolayers. *Wear* **2006,** 260, (1-2), 209-214.
8. Srinivasan, U.; Houston, M. R.; Howe, R. T.; Maboudian, R., Alkyltrichlorosilane-based self-assembled monolayer films for stiction reduction in silicon micromachines. *Journal of Microelectromechanical Systems* **1998,** 7, (2), 252-260.
9. Helmy, R.; Fadeev, A. Y., Self-assembled monolayers supported on TiO2: Comparison of C18H37SiX3 (X = H, Cl, OCH3C18H37Si(CH3)2C1, and C18H37PO(OH)(2). *Langmuir* **2002,** 18, (23), 8924-8928.
10. Wilson, K. A.; Finch, C. A.; Anderson, P.; Vollmer, F.; Hickman, J. J., Whispering gallery mode biosensor quantification of fibronectin adsorption kinetics onto alkylsilane monolayers and interpretation of resultant cellular response. *Biomaterials* **2012,** 33, (1), 225-236.
11. Wiencek, K. M.; Fletcher, M., Bacterial adhesion to hydroxyl-terminated and methyl-terminated alkanethiol self-assembled monolayers. *Journal of Bacteriology* **1995,** 177, (8), 1959-1966.
12. Baeumchen, O.; Fetzer, R.; Klos, M.; Lessel, M.; Marquant, L.; Haehl, H.; Jacobs, K., Slippage and nanorheology of thin liquid polymer films. *Journal of Physics: Condensed Matter* **2012,** 24, (32).
13. Farm, E.; Kemell, M.; Ritala, M.; Leskela, M., Selective-area atomic layer deposition with microcontact printed self-assembled octadecyltrichlorosilane monolayers as mask layers. *Thin Solid Films* **2008,** 517, (2), 972-975.
14. Gutfreund, P.; Baeumchen, O.; Fetzer, R.; van der Grinten, D.; Maccarini, M.; Jacobs, K.; Zabel, H.; Wolff, M., Solid surface structure affects liquid order at the polystyrene-self-assembled-monolayer interface. *Physical Review E* **2013,** 87, (1), 012306.
15. Vallant, T.; Kattner, J.; Brunner, H.; Mayer, U.; Hoffmann, H., Investigation of the formation and structure of self-assembled alkylsiloxane monolayers on silicon using in situ attenuated total reflection infrared spectroscopy. *Langmuir* **1999,** 15, (16), 5339-5346.
16. Unger, W. E. S.; Lippitz, A.; Gross, T.; Friedrich, J. F.; Woll, C.; Nick, L., The use of octadecyltrichlorosilane self-assembled layers as a model for the assessment of plasma treatment and metallization effects on polyolefins. *Langmuir* **1999,** 15, (4), 1161-1166.

17. Peters, R. D.; Nealey, P. F.; Crain, J. N.; Himpsel, F. J., A near edge X-ray absorption fine structure spectroscopy investigation of the structure of self-assembled films of octadecyltrichlorosilane. *Langmuir* **2002,** 18, (4), 1250-1256.
18. Ma, J. Q.; Pang, C. J.; Mo, Y. F.; Bai, M. W., Preparation and tribological properties of multiply-alkylated cyclopentane (MAC)-octadecyltrichlorosilane (OTS) double-layer film on silicon. *Wear* **2007,** 263, 1000-1007.
19. Yamamoto, H.; Watanabe, T.; Ohdomari, I., A molecular simulation study of an organosilane self-assembled monolayer/SiO(2) substrate interface. *Journal of Chemical Physics* **2008,** 128, (16), 164710.
20. Zhang, L. Z.; Wesley, K.; Jiang, S. Y., Molecular simulation study of alkyl monolayers on Si(111). *Langmuir* **2001,** 17, (20), 6275-6281.
21. Zhan, Y. J.; Xing, L.; Mattice, W. L., Simulations of self-assembled monolayers with the same surface-density but different grafting patterns. *Langmuir* **1995,** 11, (6), 2103-2108.
22. Barlow, D. J.; Muslim, A. M.; Webster, J. R. P.; Penfold, J.; Hollinshead, C. M.; Lawrence, M. J., Molecular modelling of surfactant monolayers under constraints derived from neutron reflectance measurements. *Physical Chemistry Chemical Physics* **2000,** 2, (22), 5208-5213.
23. Barriga, J.; Coto, B.; Fernandez, B., Molecular dynamics study of optimal packing structure of OTS self-assembled monolayers on SiO2 surfaces. *Tribology International* **2007,** 40, (6), 960-966.
24. Dickie, A. J.; Kakkar, A. K.; Whitehead, M. A., Molecular modelling of self-assembled alkynyl monolayer structures - Unnatural symmetry units, surface bonding, and topochemical polymerization. *Canadian Journal of Chemistry-Revue Canadienne De Chimie* **2003,** 81, (11), 1228-1240.
25. Chandross, M.; Webb, E. B.; Stevens, M. J.; Grest, G. S.; Garofalini, S. H., Systematic study of the effect of disorder on nanotribology of self-assembled monolayers. *Physical Review Letters* **2004,** 93, (16), 166103.
26. Pastorino, C.; Binder, K.; Kreer, T.; Muller, M., Static and dynamic properties of the interface between a polymer brush and a melt of identical chains. *Journal of Chemical Physics* **2006,** 124, (6), 064902.
27. Frenkel, D.; Smit, B., *Understanding Molecular Simulations: From Algorithms to Applications*. 2nd ed.; Academic Press: San Diego, 2002.
28. Pronk, S.; Pall, S.; Schulz, R.; Larsson, P.; Bjelkmar, P.; Apostolov, R.; Shirts, M. R.; Smith, J. C.; Kasson, P. M.; van der Spoel, D.; Hess, B.; Lindahl, E., GROMACS 4.5: a high-throughput and highly parallel open source molecular simulation toolkit. *Bioinformatics* **2013,** 29, (7), 845-854.
29. Booth, B. D.; Vilt, S. G.; Ben Lewis, J.; Rivera, J. L.; Buehler, E. A.; McCabe, C.; Jennings, G. K., Tribological Durability of Silane Monolayers on Silicon. *Langmuir* **2011,** 27, (10), 5909-5917.
30. Tatsumura, K.; Watanabe, T.; Yamasaki, D.; Shimura, T.; Umeno, M.; Ohdomari, I., Residual order within thermally grown amorphous SiO2 on crystalline silicon. *Physical Review B* **2004,** 69, (8).
31. Kojio, K.; Ge, S. R.; Takahara, A.; Kajiyama, T., Molecular aggregation state of n-octadecyltrichlorosilane monolayer prepared at an air/water interface. *Langmuir* **1998,** 14, (5), 971-974.

32. Wyckoff, R. W. G., Die Kristallstruktur von beta-Crystobalit Si O2 (bei hohen Temperaturen stabile Form). *Zeitschrift Fur Kristallographie* **1925,** 62, (3/4), 189-200.
33. Stevens, M. J., Thoughts on the Structure of alkylsilane monolayers. *Langmuir* **1999,** 15, (8), 2773-2778.
34. Osnis, A.; Sukenik, C. N.; Major, D. T., Structure of Carboxyl-Acid-Terminated Self-Assembled Monolayers from Molecular Dynamics Simulations and Hybrid Quantum Mechanics-Molecular Mechanics Vibrational Normal-Mode Analysis. *Journal of Physical Chemistry C* **2011,** 116, (1), 770-782.
35. Kong, Z.; Wang, Q.; Chen, E.; Wu, T., Study on preparation method for short-chain alkylsiloxane self-assembled monolayers and the diffusion behavior of copper on silica surfaces. *Applied Surface Science* **2013,** 279, 171-179.
36. Jorgensen, W. L.; Maxwell, D. S.; Tirado-Rives, J., Development and testing of the OPLS all-atom force field on conformational energetics and properties of organic liquids. *Journal of the American Chemical Society* **1996,** 118, (45), 11225-11236.
37. Lorenz, C. D.; Webb, E. B.; Stevens, M. J.; Chandross, M.; Grest, G. S., Frictional dynamics of perfluorinated self-assembled monolayers on amorphous SiO2. *Tribology Letters* **2005,** 19, (2), 93-99.
38. Bussi, G.; Donadio, D.; Parrinello, M., Canonical sampling through velocity rescaling. *Journal of Chemical Physics* **2007,** 126, (1), 014101.
39. Bondi, A., van der Waals volumes + radii. *Journal of Physical Chemistry* **1964,** 68, (3), 441-451.
40. Linford, M. R.; Fenter, P.; Eisenberger, P. M.; Chidsey, C. E. D., Alkyl monolayers on silicon prepared from 1-alkenes and hydrogen-terminated silicon. *Journal of the American Chemical Society* **1995,** 117, (11), 3145-3155.
41. Wasserman, S. R.; Tao, Y. T.; Whitesides, G. M., Structure and reactivity of alkylsiloxane monolayers formed by reaction of alkyltrichlorosilanes on silicon substrates. *Langmuir* **1989,** 5, (4), 1074-1087.
42. Bierbaum, K.; Grunze, M.; Baski, A. A.; Chi, L. F.; Schrepp, W.; Fuchs, H., Growth of self-assembled n-alkyltrichlorosilane films on Si(100) investigated by atomic-force microscopy. *Langmuir* **1995,** 11, (6), 2143-2150.
43. Garcia-Parajo, M.; Longo, C.; Servat, J.; Gorostiza, P.; Sanz, F., Nanotribological properties of octadecyltrichlorosilane self-assembled ultrathin films studied by atomic force microscopy: Contact and tapping modes. *Langmuir* **1997,** 13, (8), 2333-2339.
44. Allara, D. L.; Parikh, A. N.; Rondelez, F., Evidence for a unique chain organization in long-chain silane monolayers deposited on 2 widely different solid substrates. *Langmuir* **1995,** 11, (7), 2357-2360.
45. Calistri-Yeh, M.; Kramer, E. J.; Sharma, R.; Zhao, W.; Rafailovich, M. H.; Sokolov, J.; Brock, J. D., Thermal stability of self-assembled monolayers from alkylchlorosilanes. *Langmuir* **1996,** 12, (11), 2747-2755.
46. Tillman, N.; Ulman, A.; Schildkraut, J. S.; Penner, T. L., Incorporation of phenoxy groups in self-assembled monolayers of trichlorosilane derivatives - Effects on film thickness, wettability, and molecular-orientation. *Journal of the American Chemical Society* **1988,** 110, (18), 6136-6144.
47. Wang, M.; Liechti, K. M.; Srinivasan, V.; White, J. M.; Rossky, P. J.; Stone, M. T., A hybrid continuum-molecular analysis of interfacial force microscope experiments on a self-

assembled monolayer. *Journal of Applied Mechanics-Transactions of the Asme* **2006,** 73, (5), 769-777.
48. Tidswell, I. M.; Rabedeau, T. A.; Pershan, P. S.; Kosowsky, S. D.; Folkers, J. P.; Whitesides, G. M., X-ray grazing-incidence diffraction from alkylsiloxane monolayers on silicon-wafers. *Journal of Chemical Physics* **1991,** 95, (4), 2854-2861.
49. Schreiber, F., Structure and growth of self-assembling monolayers. *Progress in Surface Science* **2000,** 65, (5-8), 151-256.
50. Vemparala, S.; Karki, B. B.; Kalia, R. K.; Nakano, A.; Vashishta, P., Large-scale molecular dynamics simulations of alkanethiol self-assembled monolayers. *Journal of Chemical Physics* **2004,** 121, (9), 4323-4330.
51. Brunner, H.; Mayer, U.; Hoffmann, H., External reflection infrared spectroscopy of anisotropic adsorbate layers on dielectric substrates. *Applied Spectroscopy* **1997,** 51, (2), 209-217.
52. Hoffmann, H.; Mayer, U.; Krischanitz, A., Structure of alkylsiloxane monolayers on silicon surfaces investigated by external reflection infrared-spectroscopy. *Langmuir* **1995,** 11, (4), 1304-1312.
53. Kaushik, A. P.; Clancy, P., Trapping dynamics of diindenoperylene (DIP) in self-assembled monolayers using molecular simulation. *Surface Science* **2011,** 605, (13-14), 1185-1196.
54. Ewers, B. W.; Batteas, J. D., Molecular Dynamics Simulations of Alkylsilane Monolayers on Silica Nanoasperities: Impact of Surface Curvature on Monolayer Structure and Pathways for Energy Dissipation in Tribological Contacts. *Journal of Physical Chemistry C* **2012,** 116, (48), 25165-25177.
55. Tolan, M., *X-ray scattering from soft-matter thin films*. Springer: Berlin, 1999.
56. Bierbaum, K.; Kinzler, M.; Woll, C.; Grunze, M.; Hahner, G.; Heid, S.; Effenberger, F., A near-edge X-ray-absorption fine structure spectroscopy and X-ray photoelectron-spectroscopy study of the film properties of self-assembled monolayers of organosilanes on oxidized Si(100). *Langmuir* **1995,** 11, (2), 512-518.

SYNOPSIS (TOC graphic)